Osteogenic Responses to Zirconia with Hydroxyapatite Coating by Aerosol Deposition

Y. Cho[1,2,3*], J. Hong[1*], H. Ryoo[3], D. Kim[4], J. Park[5], and J. Han[1]

Abstract

Previously, we found that osteogenic responses to zirconia co-doped with niobium oxide (Nb_2O_5) or tantalum oxide (Ta_2O_5) are comparable with responses to titanium, which is widely used as a dental implant material. The present study aimed to evaluate the in vitro osteogenic potential of hydroxyapatite (HA)-coated zirconia by an aerosol deposition method for improved osseointegration. Surface analysis by scanning electron microscopy and x-ray diffraction proved that a thin as-deposited HA film on zirconia showed a shallow, regular, crater-like surface. Deposition of dense and uniform HA films was measured by SEM, and the contact angle test demonstrated improved wettability of the HA-coated surface. Confocal laser scanning microscopy indicated that MC3T3-E1 pre-osteoblast attachment did not differ notably between the titanium and zirconia surfaces; however, cells on the HA-coated zirconia exhibited a lower proliferation than those on the uncoated zirconia late in the culture. Nevertheless, ALP, alizarin red S staining, and bone marker gene expression analysis indicated good osteogenic responses on HA-coated zirconia. Our results suggest that HA-coating by aerosol deposition improves the quality of surface modification and is favorable to osteogenesis.

Keywords: implant dentistry, biomaterial(s), osteogenesis, surface chemistry, osseointegration, prosthetic dentistry

Introduction

Titanium (Ti) is a well-established dental implant material with many documented clinical successes (Buser et al. 2012). The main advantageous properties of titanium are its biocompatibility and strength under bite-force loading conditions; however, it produces a visible gray color in the soft tissues, making it esthetically unpleasant (Sailer et al. 2007). Consequently, tooth-colored biocompatible ceramics and bioactive glass substrates have been developed as novel candidate implant materials (Kaur et al. 2014). Zirconia (Zr) is osteoconductive and chemically inert, and produces a milder inflammatory response than does titanium (Hisbergues et al. 2009). Y_2O_3-stabilized tetragonal zirconia polycrystals (Y-TZP) have several advantages over other ceramics, including high fracture toughness and flexural strength (Pittayachawan et al. 2009), and have been widely used for hip replacements. However, reports of clinical failures caused by low-temperature degradation (LTD) indicated a need to improve the structural stability of this material (Gremillard and Chevalier 2008; Lughi and Sergo 2010). Modifications of zirconia with tantalum oxide (Ta_2O_5) or niobium oxide (Nb_2O_5) have been developed to prevent LTD by phase transformation from the tetragonal to the monoclinic form (Piconi and Maccauro 1999; Kim et al.

2000). Recently, we reported that tetragonal zirconia polycrystal (TZP) discs containing Y_2O_3/Ta_2O_5 or Y_2O_3/Nb_2O_5 [(Y, Ta)-TZP and (Y, Nb)-TZP, respectively] had osteogenic potential similar to that of those grown on anodized titanium, which is widely used as a dental implant material

[1]Department of Prosthodontics, School of Dentistry and Dental Research Institute, BK21 Program, Seoul National University, Seoul, Korea
[2]Department of Periodontology, School of Dentistry and Dental Research Institute, BK21 Program, Seoul National University, Seoul, Korea
[3]Department of Molecular Genetics, School of Dentistry and Dental Research Institute, BK21 Program, Seoul National University, Seoul, Korea
[4]Department of Advanced Materials Engineering, Sejong University, Seoul, Korea
[5]R&D Center, Nano Business, IONES Co., Ltd., Gyeonggi-do, Korea
*Authors contributing equally to this article.

Corresponding Author:
J. Han, Department of Prosthodontics, School of Dentistry, Seoul National University, 28 Yeongeon-dong, Jongno-gu, Seoul, Korea, 110-749.
Email: proshan@snu.ac.kr

(Cho et al. 2014). Material composition and surface topography are critical modulators of osseointegration. Accordingly, various surface modifications have been developed to enhance bone healing, including mechanical modifications such as grooves or textured rough patterns (Orsini et al. 2000; Gahlert et al. 2007; Hsu et al. 2007) and coating with biomaterials or biomolecules to induce osteogenesis (Burr et al. 1993; Aldini et al. 2002; Knabe et al. 2004; De Maeztu et al. 2008).

HA is the natural mineral form of calcium apatite, the main component of bones and teeth. Therefore, it is widely accepted as a graft material for the treatment of bone defects and as a coating material to promote osteogenesis. Thus, HA was the first material used for osseointegration in dental implants (Ogiso et al. 1992; Knabe et al. 2004; Mistry et al. 2011), although its use is controversial, because HA-coated implants have been poorly characterized (Ong and Chan 2000). Furthermore, poor-quality coatings limit the utility of HA, causing failures in bone healing and implantation. HA surface-coating methods include plasma-spraying, electrophoretic deposition, dip-coating, and spin-coating (Lee and Aoki 1995; Kuroda et al. 2002; Tamura et al. 2006; Han et al. 2008). It is difficult to produce a crystalline HA-coated surface with controlled pore size and porosity. In the present study, we introduced an aerosol deposition technique to produce a high-quality HA-coating on zirconia surfaces and to overcome the drawbacks of HA-coating (Akedo and Lebedev 2000; Akedo 2006). The objective of this study was to evaluate the surface characteristics of HA-coated surfaces by a novel aerosol deposition technique and to identify osteogenic responses to the HA-coated zirconia.

Materials and Methods

Specimen Preparation

Pure titanium discs (25 mm diameter, 1 mm thickness) were prepared by machining (Ti-machined; Ti-m) or treated by anodizing (Ti-anodizing; Ti-a) (OnePlant System, Warrantec, Seoul, Korea). Zirconia was prepared by mixing 90.6 mol% ZrO_2, 5.3 mol% Y_2O_3, and 4.1 mol% Nb_2O_5 powders for (Y, Nb)-TZP, and 86.2 mol% ZrO_2, 7.2 mol% Y_2O_3, and 6.6 mol% Ta_2O_5 for (Y, Ta)-YZP. The compositions were selected based on the absence of low-temperature degradation and the presence of reasonably high fracture toughness. Green, disc-shaped compacts (15 mm diameter, 1 mm thickness) were prepared by cold isostatic pressing of the powder mixtures at 200 MPa followed by sintering for 5 h at 1,650°C in air. The zirconia discs were polished and finished with diamond pastes to generate a mirror-like surface. After being polished, the (Y, Nb)-TZP and (Y, Ta)-TZP surfaces were roughened by sandblasting with 50 μm Al_2O_3 at 2 bar and 1 bar pressure, respectively, as we previously reported (Cho et al. 2014).

Fabrication of HA Film by Aerosol Deposition

Commercially available HA powder (CodeBio, Cheonan, Korea) was used as the starting raw material for aerosol deposition (AD) (Akedo and Lebedev 2000; Akedo 2006). The HA was annealed at 700°C for 2 h under an air atmosphere. Sandblasted (Y, Nb)-TZP and (Y, Ta)-TZP were ultrasonically cleaned with distilled water and acetone. The equipment used for AD of HA was primarily composed of an aerosol chamber and a processing chamber, connected by a tube (supplemental data). Preheated HA powders were mixed with carrier gas and aerosolized by means of a vibration system. The aerosol was added to the coating chamber through the tube and accelerated through a slit nozzle by pressure differences between the 2 chambers. The accelerated HA powder was ejected from the slit nozzle and deposited onto the discs at room temperature, to a thickness of approximately 10 μm.

Surface Roughness and Interface

The average surface roughness (R_a) and topography were measured by confocal laser scanning microscopy (CLSM; LSM700, Carl Zeiss, Oberkochen, Germany). The microstructure of the zirconia discs with and without HA-coating was observed by scanning electron microscopy (SEM; SNE-4500M, SEC CO., LTD, Suwon, Korea). In addition to this, interfaces between HA films and zirconia discs were observed by SEM to confirm deposition of dense HA films. R_a values represent the mean ± SD of 3 independent experiments.

Contact Angle

Four uncoated zirconia discs and HA-coated zirconia discs were prepared. Distilled water at 36.5°C was dropped onto each of the discs, and 5 s later, contact angles were measured by means of an automated contact-angle-measuring device (Phoenix300, S.E.O. Co., Ltd., Ansung, Korea). Values represent the mean ± SD of 3 independent experiments.

Crystallinity

X-ray diffraction (XRD; MiniFlex 600; Rigaku CO., LTD, Tokyo, Japan) was used to examine the crystal structure of the deposited HA layer. XRD data were matched with Joint Committee on Powder Diffraction Standards (JCPDS) card # 9-432.

Cell Culture

Mouse pre-osteoblast MC3T3-E1 cells were purchased from ATCC (Manassas, VA, USA), seeded onto the discs, and cultured in α-minimal essential medium (α-MEM, Logan, UT, USA) with 10% fetal bovine serum (FBS) and 1% penicillin/streptomycin. Trypsinized and resuspended

cells were seeded onto the discs at a density 1 x 10^4 cells/cm^2 and incubated in air at 37°C and 5% CO_2. Three specimens were statically cultured per time interval, and 3 sets of cultures were examined for all in vitro experiments. The osteogenic medium contained 10 mM β-glycerophosphate and 50 μg/mL ascorbic acid in the α-MEM.

Cell Attachment

Twenty-four h after being seeded, disc-adherent cells were fixed in 4% formaldehyde. 4′,6-diamidino-2-phenylindole (DAPI; Invitrogen, Carlsbad, CA, USA) and Alexa Fluor 568 phalloidin (Invitrogen, Carlsbad, CA, USA) were used for detection of the nucleus and cytoskeleton, respectively. Fluorescence was visualized by CLSM and analyzed with ZEN2011 software (Carl Zeiss, Oberkochen, Germany).

Cell Proliferation Assay

At 1, 4, and 7 d after seeding, following attachment, picogreen assays were performed with a Quant-iT PicoGreen assay kit (Invitrogen Ltd., Paisley, UK) for the assessment of cellular proliferation. MC3T3-E1 cells (1 x 10^4 cells/cm^2) were seeded onto the discs. Disc-adherent cells were washed with phosphate-buffered saline (PBS) and subjected to lysis with Tris-ethylenediaminetetraacetic acid (EDTA; TE) buffer (10 mM Tris-HCl, 1 mM EDTA, pH 7.5). DNA contents were determined by mixing 100 μL of picogreen reagent with 100 μL of DNA sample. The samples were loaded in triplicate, and fluorescence intensity was measured with a GloMax Multi-Detection System (Promega, Madison, WI, USA). Fluorescence intensity was converted to DNA concentration using a DNA standard curve according to the manufacturer's protocol. Values represent the mean ± SD of 3 independent experiments.

Cytotoxicity Test

Cytotoxicity was measured with Cell Counting Kit-8 (CCK-8; Dojindo, Tokyo, Japan). MC3T3-E1 cells (1 x 10^4 cells/cm^2) were plated onto the discs, and tests were performed at 1, 4, and 7 d after seeding. CCK-8 solution was added to each well, followed by incubation for 2 h at 37°C. The absorbance at 450 nm was determined by a GloMax Multi-Detection System (Promega, Madison, WI, USA). Values represent the mean ± SD of 3 independent experiments.

Reverse-transcription PCR and Quantitative Real-time PCR

Cells were harvested at 2, 6, 10, and 15 d after osteoblast differentiation. RNA was isolated with QIAzol lysis reagent (QIAGEN, Valencia, CA, USA). The Primescript™ RT reagent kit for reverse transcription was purchased from

Takara (Shiga, Japan). Quantitative real-time PCR was performed with primer sets for type I collagen (*Col1A1*), alkaline phosphatase (*Alp*), and osteocalcin (*Oc*) as previously described (Cho et al. 2009) and with Takara SYBR premix Ex Taq (Takara) on a 7500 Real-Time PCR system (Applied Biosystems, Foster City, CA, USA). The PCR primers were synthesized by Integrated DNA Technology (Coralville, IA, USA). All samples were run in duplicate, and the relative expression levels were normalized to glyceraldehyde-3-phosphate dehydrogenase (*Gapdh*). *Gapdh* mRNA expression levels remained steady during osteoblast differentiation, showing similar Ct values. Values represent the mean ± SD of 3 independent experiments.

Alkaline Phosphatase (ALP) Staining

An ALP staining kit was purchased from Sigma-Aldrich (St. Louis, MO, USA). Cells were cultured in osteogenic medium for 7 d, washed twice with PBS, and stained as described by the manufacturer.

Alizarin Red S Staining

Cells were cultured in osteogenic medium for 21 d and washed twice with phosphate-buffered saline, fixed with 70% ethanol for 1 h, washed twice with distilled water, and stained with 40 mM alizarin red S (Sigma-Aldrich, St. Louis, MO, USA) for 10 min, then washed 3 times with distilled water.

Statistical Analysis

All quantitative data are presented as the mean ± SD. Each experiment was performed at least 3 times, and the results from one representative experiment are shown. Student's *t* test was used for the contact angle and R_a value. Statistical analyses for cell proliferation assay, cytotoxicity test, and quantitative real-time PCR were performed by one-way analysis of variance (ANOVA) with Tukey's post hoc test. Post hoc analysis was used to detect pairs of groups with statistically significant differences. Significance was considered at $P < 0.05$ (SPSS, Chicago, IL, USA).

Results

Characterization of the HA Film

HA film was produced and optimized using HA powder with a particle size of approximately 0.8–1.1 μm. The XRD patterns of the raw HA powder before deposition (raw), the heat-treated HA powder (700°C), and the as-deposited HA film (as-deposited) are shown in Fig. 1A (labeled a, b, and c, respectively). The peaks of the HA powder were consistent with the dominant peaks of pure HA with high
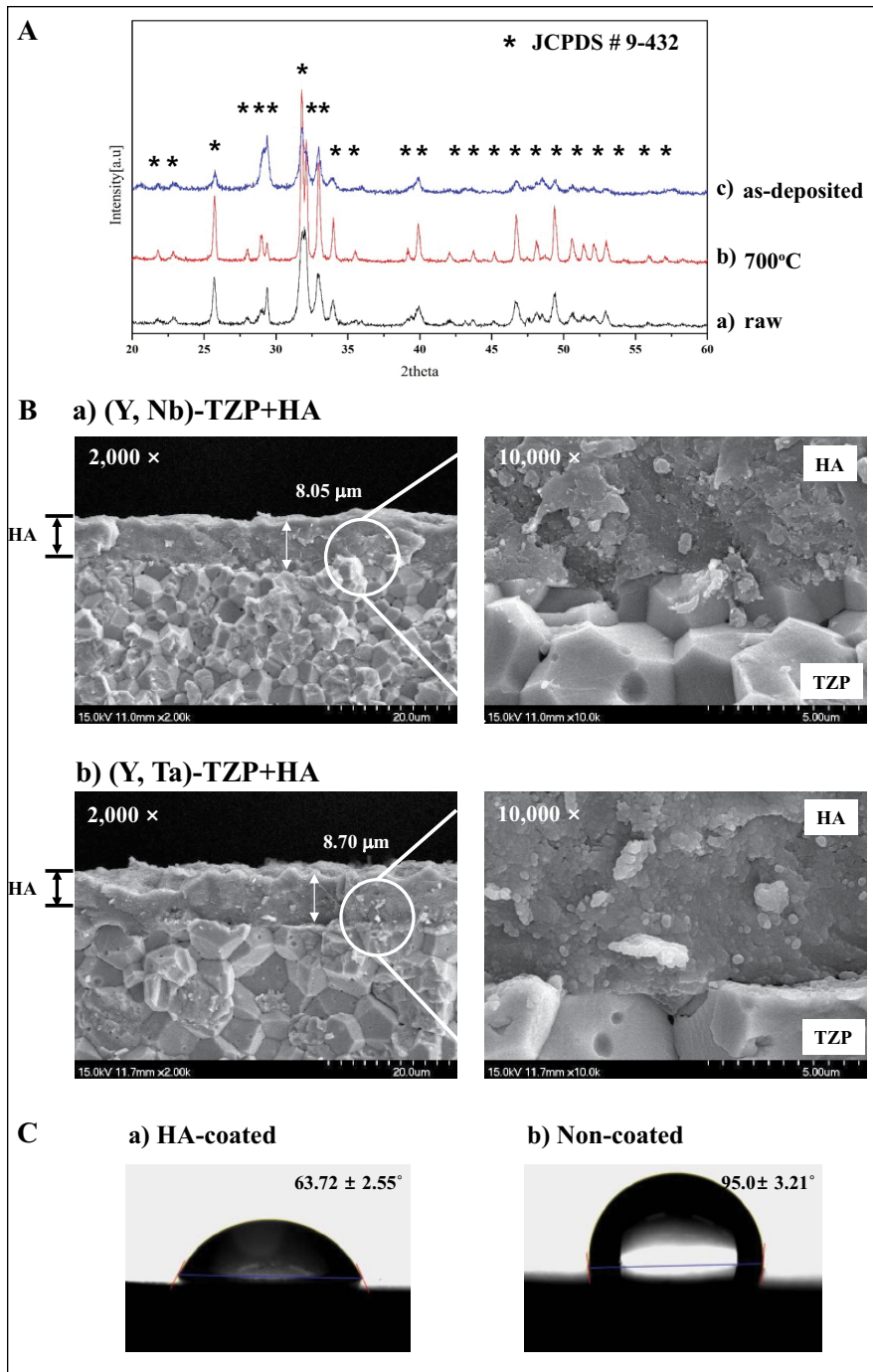
Figure 1. Surface analysis of hydroxyapatite (HA)-coated zirconia. (**A**) X-ray diffraction (XRD) patterns of raw HA powder before deposition (a), heat-treated HA powder (b), and as-deposited HA film (c) on the zirconia discs. (**B**) The cross-sections of the deposited HA film [HA-coated (Y, Nb)-TZP (a) and HA-coated (Y, Ta)-TZP (b)] were observed by scanning electron microscopy (SEM). Images are magnified 2,000× (left) and 10,000× (right). (**C**) Contact angle between the water drop and the substratum: (a) HA-coated zirconia surface and (b) non-coated zirconia surface.

crystallinity (asterisk, Fig. 1A). XRD analysis revealed only HA peaks (JCPDS card # 9-432). Collectively, the HA

film exhibited only pure HA peaks without secondary crystalline phases. Thus, the composition of the powder and film indicated that no chemical changes had occurred during deposition. The cross-section of HA films on the (Y, Nb)-TZP (a) and (Y, Ta)-TZP (b) was observed by SEM (Fig. 1B). There were no pores and cracks in the film layers, indicating the deposition of fully dense HA films. The deposited HA films had no orientation and showed round particles, because the raw HA particles for aerosol deposition were round. The thickness of HA films averaged 8.05 and 8.70 μm on (Y, Nb)-TZP and (Y, Ta)-TZP discs, respectively, and the thickness of all experimental specimens was well-maintained in this study. The contact angle was significantly lower for HA-coated surfaces (a, $63.72 \pm 2.55°$, $P < 0.001$; Fig. 1C) than for non-coated zirconia surfaces (b, $95.0 \pm 3.21°$, $P < 0.001$; Fig. 1C).

Surface Analysis of HA Film on Zirconia by AD

For each specimen, the average roughness (R_a) and surface topography were analyzed by CLSM. The R_a values of the (Y, Nb)-TZP and HA-coated (Y, Nb)-TZP were 0.819 ± 0.05 μm and 1.131 ± 0.12 μm, respectively (Figs. 2A, B, upper panel). The R_a values of the (Y, Ta)-TZP and HA-coated (Y, Ta)-TZP surfaces were 0.880 ± 0.06 μm and 1.004 ± 0.12 μm, respectively (Figs. 2C, D, upper panel). A significant increase was observed in surface roughness with HA coating ($P < 0.05$). The surface morphology was observed by SEM (Figs. 2A–D, bottom panel). As-deposited HA film on the discs produced a shallow crater-like surface with a network-type microstructure (Figs. 2B, D, bottom panel) and increased surface roughness.
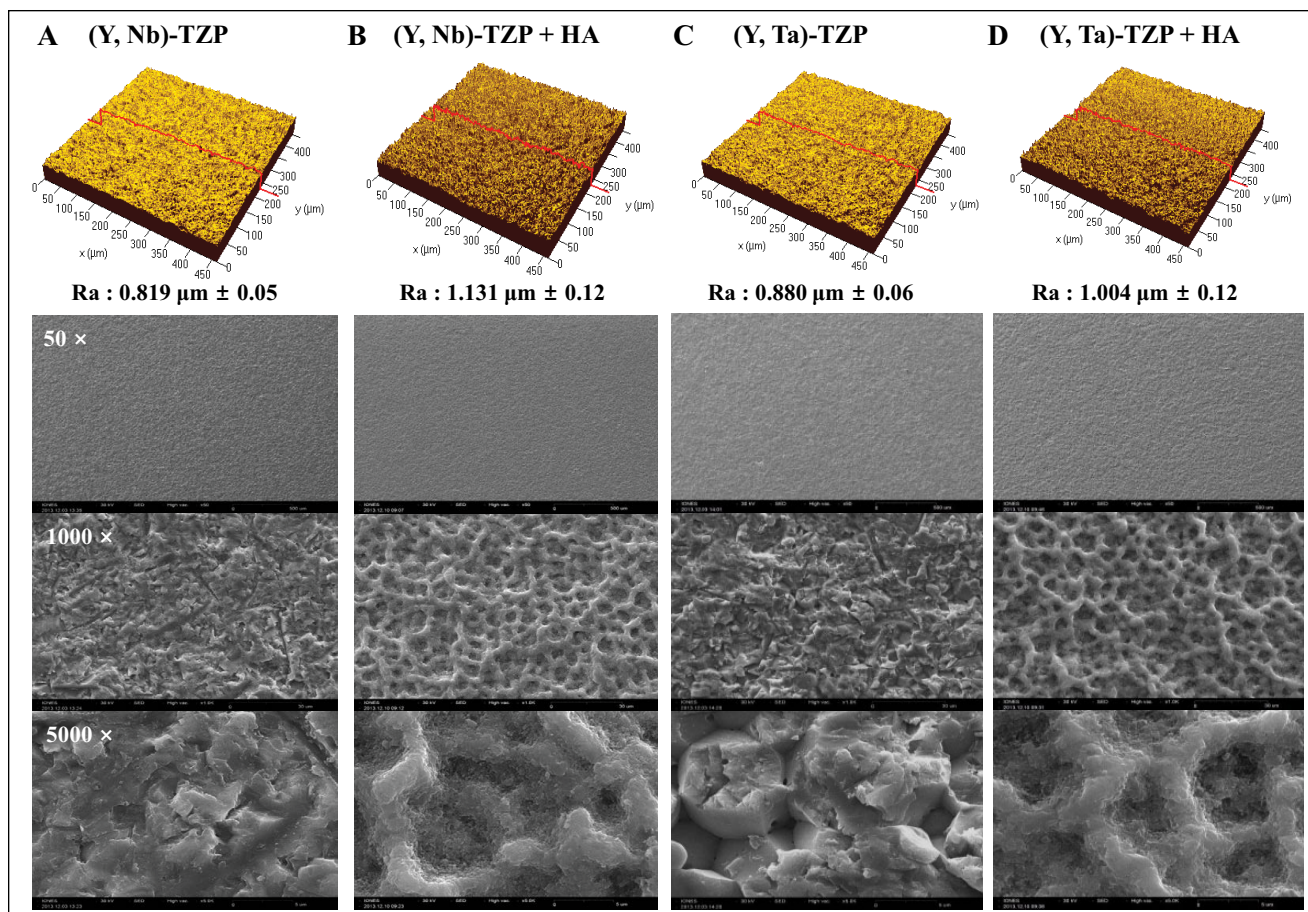
Figure 2. Confocal laser scanning microscopy (CLSM) images showing the roughness (R_a) of the material surfaces (upper panel). (**A**) (Y, Nb)-TZP; (**B**) hydroxyapatite (HA)-coated (Y, Nb)-TZP; (**C**) (Y, Ta)-TZP; and (**D**) HA-coated (Y, Ta)-TZP. Scanning electron microscopy (SEM) images of material surfaces (A-D, bottom panel). Images are magnified 50×, 1,000×, and 5,000×.

Cell Attachment and Morphology

We examined cell attachment and morphology by CLSM 24 h after seeding MC3T3-E1 pre-osteoblast cells onto the discs (Fig. 3). Cell adhesion to the (Y, Nb)-TZP (Fig. 3C) and (Y, Ta)-TZP (Fig. 3E) discs was similar to adhesion to the Ti-m (Fig. 3A) and Ti-a (Fig. 3B) discs. However, cells on the HA-coated (Y, Nb)-TZP (Fig. 3D) and HA-coated (Y, Ta)-TZP (Fig. 3F) discs exhibited unusual morphology, with an elongated and thin cytoskeletal appearance.

Cellular Proliferation and Viability

Cellular proliferation on the zirconia and titanium discs was analyzed by picogreen assay (Fig. 4A). Cells were seeded and cultured on the discs and harvested at 1, 4, and 7 d. The proliferation increased throughout the experiment; cells proliferated more efficiently on the polished surfaces (Ti-m) than on the rough surfaces [Ti-a, (Y, Nb)-TZP ± HA, and (Y, Ta)-TZP ± HA]. Although the cell morphology suggested

otherwise, cells on the HA-coated zirconia discs proliferated well, although more slowly than those on the uncoated discs. We also tried the CCK-8 assay for cell viability, and results agreed with those of the picogreen assay (Fig. 4B). These results suggest that HA coating is not cytotoxic; thus, it is biocompatible.

Osteoblast Differentiation

MC3T3-E1 pre-osteoblast cells were harvested after 2, 6, 10, and 15 d of differentiation, and real-time PCR was performed to measure the expression of the bone marker genes *Col1A1* (Fig. 5A), *Alp* (Fig. 5B), and *Oc* (Fig. 5C) (Cho et al. 2009). Although the osteoblast differentiation patterns were similar, the degree of differentiation varied slightly among the surfaces. The polished Ti-m surface had a lower differentiation capacity than did the rough surfaces (Ti-a). Notably, HA-coated (Y, Nb)-TZP and HA-coated (Y, Ta)-TZP discs exhibited osteogenic responses that were equivalent to or slightly high than that of Ti-a, which is well-known
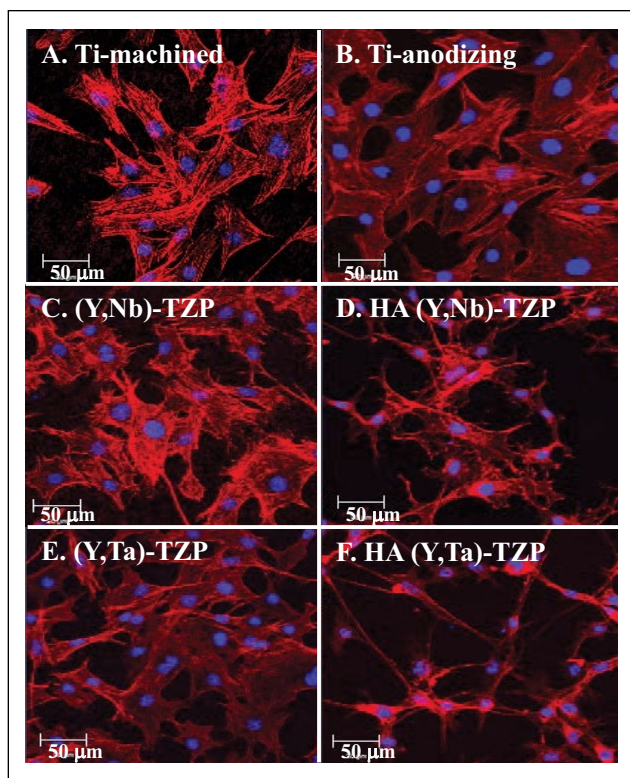
Figure 3. Confocal images of MC3T3-E1 cells 24 h after being seeded onto titanium (Ti) or zirconia (Zr) discs. (**A**) Titanium-machined, (**B**) titanium-anodized, (**C**) sandblasted (Y, Nb)-TZP, (**D**) hydroxyapatite (HA)-coated (Y, Nb)-TZP, (**E**) sandblasted (Y, Ta)-TZP, and (**F**) HA-coated (Y, Ta)-TZP. Original magnification is 300×; bar = 50 μm.

for its efficacy in dental osseointegration. To verify the osteogenic effects of HA-coated zirconia, we performed ALP staining (Fig. 5D) and alizarin red S staining (Fig. 5E), which showed that the HA-coated (Y, Nb)-TZP and HA-coated (Y, Ta)-TZP discs had better osteogenic potential than did the uncoated zirconia discs.

Discussion

In the present work, we present a novel method for depositing HA film by aerosol deposition (AD). HA-coating was first introduced in the 1980s for improved osseointegration between bone and implants (Furlong and Osborn 1991). Many studies have focused on the osteogenic response to the HA-coating interface, as well as on the problems associated with the coating method and optimization of coating properties for the best biocompatibility and osseointegration (Ong and Chan 2000; Sun et al. 2001; Wang et al. 2006). Several HA-coating methods have been introduced. Among them, plasma-spraying is commercially the most frequently used method and has shown many advantages in
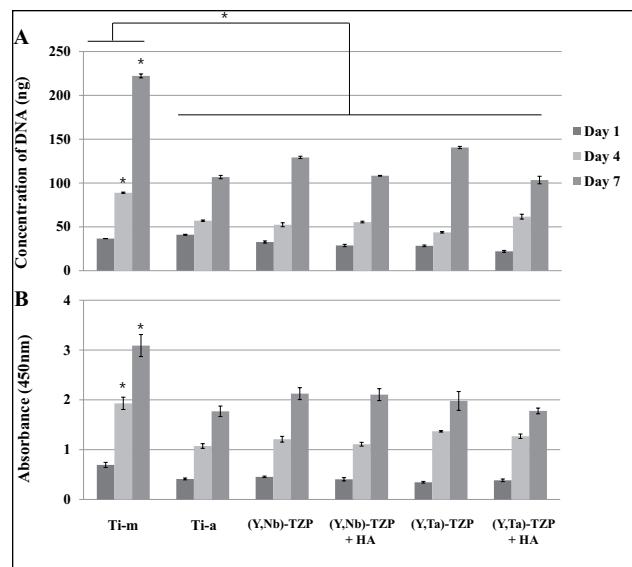
Figure 4. Cellular proliferation and viability on the discs. (**A**) Picogreen assay. Proliferation of MC3T3-E1 cells on titanium (Ti) or zirconia (Zr) discs on days 1, 4, and 7. (**B**) CCK-8 assay. Cell viability was tested on days 1, 4, and 7 under the same conditions with picogreen assay. The data are expressed as the mean ± SD of 3 independent experiments. *Significant differences between groups ($P < 0.05$).

bone tissue response. However, despite the successful results, disadvantages such as irregular thickness, variations in crystallinity and composition of the coating, and exfoliation of the coating layer have been reported. Therefore, it is important to ensure that the coating layer is uniform, and that crystallinity or composition does not change.

Surface analysis in the present study confirmed that the specimens had uniform and dense HA-coating thickness, improved wettability, and improved surface roughness. Analysis of our XRD data showed slightly weaker and broadened HA peaks of the films in comparison with those of the original HA powder (Fig. 1A). The presence of weak, broadened XRD peaks might suggest a small crystallite size of the coating; however, it is well-known that these phenomena can be induced by the high-energy impact of the powder particles on the substrate during the AD process (Akedo 2006). In the present study, the HA-coating layer was composed of dense and uniform crystalline without a creation of amorphous HA, and hence it can be suggested that aerosol deposition will be highly resistant to dissolution, which is a drawback of HA-coating. Surface hydrophilicity has been known to influence osseointegration. The HA-coating in our study reduced the contact angle significantly and induced hydrophilicity (Fig. 1C). As is well-known, rapid hydration of the surface could enhance cell adhesion and bone apposition (Rupp et al. 2006). Therefore, we suggest, based on analysis of our data, that the enhanced wettability in the HA-coated surface would have a good

influence on osseointegration. Many review articles have reported on the positive relationship between surface roughness and osseointegration (Shalabi et al. 2006; Le Guéhennec et al. 2007; Wennerberg and Albrektsson 2010). Based on these, many trials for creating suitable surface roughness were conducted with the inclusion of HA-coating. Analysis of SEM data showed that the HA-coating formed a rough surface with a porous network-type microstructure and improved the R_a value of the zirconia discs (Fig. 2).

Excellent osseointegration is the final goal of bone tissue healing around implant materials. HA must induce an appropriate cellular response to ensure biocompatibility and bioactivity and to promote osseointegration between bone and implant with good-quality coating. In this study, HA deposition induced a slight stress response in adherent cells, observed as a de-bulked and elongated cytoskeleton (Figs. 3D, F). Moreover, while HA did not affect proliferation at 4 d of cell culture, proliferation was slightly lower than on the uncoated surfaces by day 7 (Fig. 4). This apparent phenomenon has been demonstrated elsewhere in vitro, whereas an in vivo study showed early tissue integration (Roy et al. 2011). Despite the slight stressful state that was observed on the HA-coated zirconia in the present study (Figs. 3, 4), real-time PCR and staining showed that the cells were well-differentiated on HA-coated zirconia surfaces (Fig. 5). Many other in vitro and in vivo studies have reported the benefits of HA deposition on implants (Chang et al. 1999; Rigo et al. 2004; Yang et al. 2009); however, HA coatings also present problems, such as dissolution of the HA and bacterial susceptibility (Ong and Chan 2000). Thus, improving the clinical usefulness of HA in dental implant materials remains a priority for future studies.

Taken together, our novel HA-coating method by aerosol deposition can be used to apply a thin and uniform coating of highly crystalline HA over zirconia implants, with good wettability. Furthermore, our in vitro study demonstrated
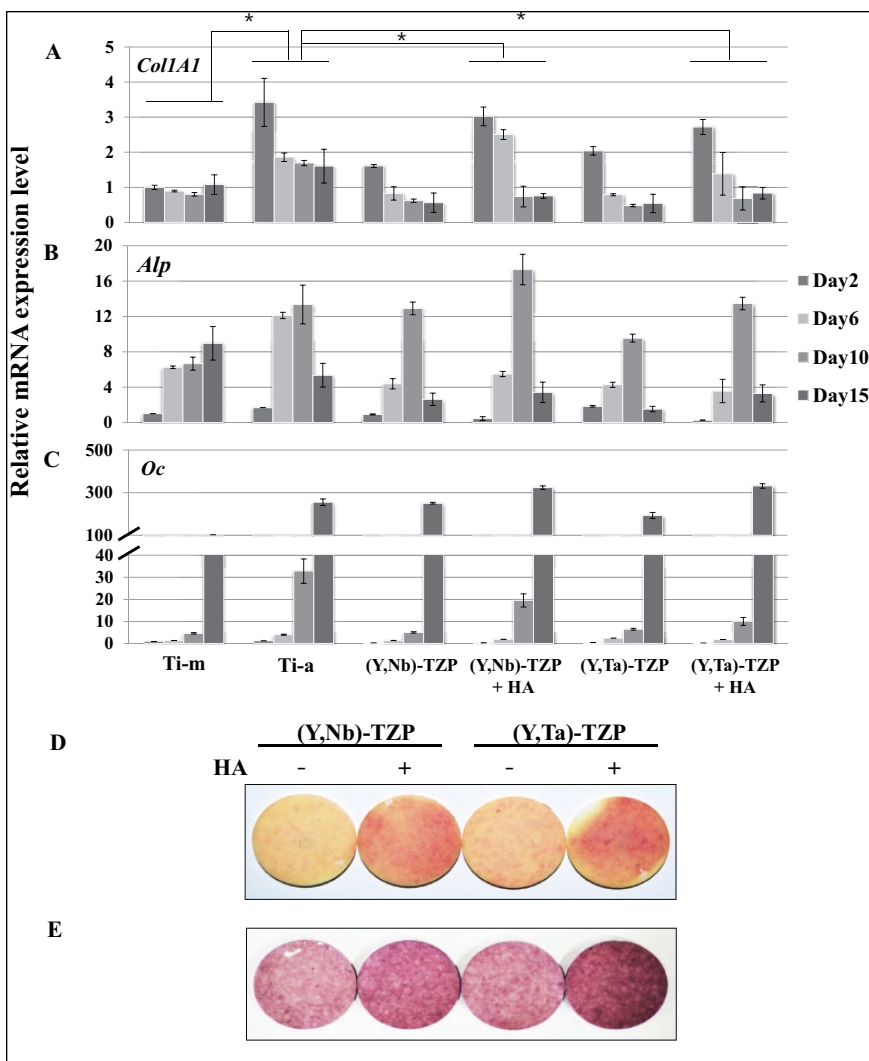
Figure 5. Real-time PCR. (**A**) Type I collagen (*Col1A1*), (**B**) alkaline phosphatase (*Alp*), and (**C**) osteocalcin (*Oc*) in MC3T3-E1 cells on titanium (Ti) or zirconia (Zr) discs after 2, 6, 10, and 15 d of culture in osteogenic medium. The data are expressed as the mean ± SD of 3 independent experiments. *Significant differences between groups ($P < 0.05$). (**D**) ALP staining. Cells were seeded onto the discs and cultured in osteogenic medium for 7 d. ALP activity was determined by cytochemical staining as indicated in "Materials and Methods," (**E**) Alizarin red S staining. Cells were seeded onto the discs and cultured in osteogenic medium for 21 d. Staining procedure is described in "Materials and Methods."

that HA coating could be used for the method of implant surface modification showing favorable osteogenic response. However, further in vivo study is needed to confirm the efficacy of HA-coated zirconia implants with respect to osseointegration.

Author Contributions

Y.D. Cho, J.S. Han, contributed to conception, design, data acquisition, analysis, and interpretation, drafted and critically revised the manuscript; J.S. Hong, contributed to conception, data acquisition,

and analysis, drafted the manuscript; H.M. Ryoo, contributed to conception and data analysis, drafted the manuscript; D.J. Kim, J.H. Park, contributed to design and data analysis, drafted the manuscript. All authors gave final approval and agree to be accountable for all aspects of the work.

Acknowledgments

References

Akedo J, Lebedev M. 2000. Piezoelectric properties and poling effect of Pb(Zr, Ti)O-3 thick films prepared for microactuators by aerosol deposition. Appl Phys Lett. 77:1710–1712.

Akedo J. 2006. Aerosol deposition of ceramic thick films at room temperature: densification mechanism of ceramic layers. J Am Ceram Soc. 89(6):1834–1839.

Aldini NN, Fini M, Giavaresi G, Torricelli P, Martini L, Giardino R, Ravaglioli A, Krajewski A, Mazzocchi M, Dubini B, et al. 2002. Improvement in zirconia osseointegration by means of a biological glass coating: an in vitro and in vivo investigation. J Biomed Mater Res. 61(2):282–289.

Burr DB, Mori S, Boyd RD, Sun TC, Blaha JD, Lane L, Parr J. 1993. Histomorphometric assessment of the mechanisms for rapid ingrowth of bone to HA/TCP coated implants. J Biomed Mater Res. 27(5):645–653.

Buser D, Janner SF, Wittneben JG, Brägger U, Ramseier CA, Salvi GE. 2012. 10-year survival and success rates of 511 titanium implants with a sandblasted and acid-etched surface: a retrospective study in 303 partially edentulous patients. Clin Implant Dent Relat Res. 14(6):839–851.

Chang YL, Stanford CM, Wefel JS, Keller JC. 1999. Osteoblastic cell attachment to hydroxyapatite-coated implant surfaces in vitro. Int J Oral Maxillofac Implants. 14(2):239–247.

Cho YD, Yoon WJ, Woo KM, Baek JH, Lee G, Cho JY, Ryoo HM. 2009. Molecular regulation of matrix extracellular phosphoglycoprotein expression by bone morphogenetic protein-2. J Biol Chem. 284(37):25230–25240.

Cho YD, Shin JC, Kim HL, Gerelmaa M, Yoon HI, Ryoo HM, Kim DJ, Han JS. 2014. Comparison of the osteogenic potential of titanium- and modified zirconia-based bioceramics. Int J Mol Sci. 15(3):4442–4452.

De Maeztu MA, Braceras I, Alava JI, Gay-Escoda C. 2008. Improvement of osseointegration of titanium dental implant surfaces modified with CO ions: a comparative histomorphometric study in beagle dogs. Int J Oral Maxillofac Surg. 37(5):441–447.

Furlong RJ, Osborn JF. 1991. Fixation of hip prostheses by hydroxyapatite ceramic coatings. J Bone Joint Surg Br. 73(5):741–745.

Gahlert M, Gudehus T, Eichhorn S, Steinhauser E, Kniha H, Erhardt W. 2007. Biomechanical and histomorphometric comparison between zirconia implants with varying surface textures and a titanium implant in the maxilla of miniature pigs. Clin Oral Implants Res. 18(5):662–668.

Gremillard L, Chevalier J (2008). Durability of zirconia-based ceramics and composites for total hip replacement. Key Engineering Materials. (361-363):791–794.

Han JY, Yu ZT, Zhou L. 2008. Hydroxyapatite/titania composite bioactivity coating processed by the sol-gel method. Biomed Mater. 3(4):044109.

Hisbergues M, Vendeville S, Vendeville P. 2009. Zirconia: established facts and perspectives for a biomaterial in dental implantology. J Biomed Mater Res B Appl Biomater. 88(2):519–529.

Hsu SH, Liu BS, Lin WH, Chiang HC, Huang SC, Cheng SS. 2007. Characterization and biocompatibility of a titanium dental implant with a laser irradiated and dual-acid etched surface. Biomed Mater Eng. 17(1):53–68.

Kaur G, Pandey OP, Singh K, Homa D, Scott B, Pickrell G. 2014. A review of bioactive glasses: their structure, properties, fabrication, and apatite formation. J Biomed Mater Res A. 102:254–274.

Kim DJ, Lee MH, Lee DY, Han JS. 2000. Mechanical properties, phase stability, and biocompatibility of (Y,Nb)-TZP/Al2O3 composite abutments for dental implant. J Biomed Mater Res. 53(4):438–443.

Knabe C, Howlett CR, Klar F, Zreiqat H. 2004. The effect of different titanium and hydroxyapatite-coated dental implant surfaces on phenotypic expression of human bone-derived cells. J Biomed Mater Res A. 71(1):98–107.

Kuroda K, Ichino R, Okido M, Takai O. 2002. Hydroxyapatite coating on titanium by thermal substrate method in aqueous solution. J Biomed Mater Res. 59(2):390–397.

Le Guéhennec L, Soueidan A, Layrolle P, Amouriq Y. 2007. Surface treatments of titanium dental implants for rapid osseointegration. Dent Mater. 23(7):844–854.

Lee J, Aoki H. 1995. Hydroxyapatite coating on Ti plate by a dipping method. Biomed Mater Eng. 5(2):49–58.

Lughi V, Sergo V. 2010. Low temperature degradation - aging - of zirconia: a critical review of the relevant aspects in dentistry. Dent Mater. 26(8):807–820.

Mistry S, Kundu D, Datta S, Basu D, Soundrapandian C. 2011. Indigenous hydroxyapatite coated and bioactive glass coated titanium dental implant system - Fabrication and application in humans. J Indian Soc Periodontol. 15(3):215–220.

Ogiso M, Tabata T, Ichijo T, Borgese D. 1992. Examination of human bone surrounded by a dense hydroxyapatite dental implant after long-term use. J Long Term Eff Med Implants. 2(4):235–247.

Ong JL, Chan DC. 2000. Hydroxyapatite and their use as coatings in dental implants: a review. Crit Rev Biomed Eng. 28(5-6):667–707.

Orsini G, Assenza B, Scarano A, Piattelli M, Piattelli A. 2000. Surface analysis of machined versus sandblasted and acid-etched titanium implants. Int J Oral Maxillofac Implants. 15(6):779–784.

Piconi C, Maccauro G. 1999. Zirconia as a ceramic biomaterial. Biomaterials. 20(1):1–25.

Pittayachawan P, McDonald A, Young A, Knowles JC. 2009. Flexural strength, fatigue life, and stress-induced phase

transformation study of Y-TZP dental ceramic. J Biomed Mater Res B Appl Biomater. 88(2):366–377.

Rigo EC, Boschi AO, Yoshimoto M, Allegrini S, Konig B, Carbonari MJ. 2004. Evaluation in vitro and in vivo of biomimetic hydroxyapatite coated on titanium dental implants. Mater Sci Eng C-Biomimet Supramolec Syst. 24(5):647–651.

Roy M, Bandyopadhyay A, Bose S. 2011. Induction plasma sprayed nano hydroxyapatite coatings on titanium for orthopaedic and dental implants. Surf Coat Technol. 205(8–9):2785–2792.

Rupp F, Scheideler L, Olshanska N, de Wild M, Wieland M, Geis-Gerstorfer J. 2006. Enhancing surface free energy and hydrophilicity through chemical modification of microstructured titanium implant surfaces. J Biomed Mater Res A. 76(2):323–334.

Sailer I, Zembic A, Jung RE, Hämmerle CH, Mattiola A. 2007. Single-tooth implant reconstructions: esthetic factors influencing the decision between titanium and zirconia abutments in anterior regions. Eur J Esthet Dent. 2(3):296–310.

Shalabi MM, Gortemaker A, Van't Hof MA, Jansen JA, Creugers NH. 2006. Implant surface roughness and bone healing: a systematic review. J Dent Res. 85(6):496–500. [Erratum in J Dent Res 2006;85(7):670.]

Sun L, Berndt CC, Gross KA, Kucuk A. 2001. Material fundamentals and clinical performance of plasma-sprayed hydroxyapatite coatings: a review. J Biomed Mater Res. 58(5):570–592.

Tamura M, Endo K, Maida T, Ohno H. 2006. Hydroxyapatite film coating by thermally induced liquid-phase deposition method for titanium implants. Dent Mater. 25(1):32–38.

Wang H, Eliaz N, Xiang Z, Hsu HP, Spector M, Hobbs LW. 2006. Early bone apposition in vivo on plasma-sprayed and electrochemically deposited hydroxyapatite coatings on titanium alloy. Biomaterials. 27(23):4192–4203.

Wennerberg A, Albrektsson T. 2010. On implant surfaces: a review of current knowledge and opinions. Int J Oral Maxillofac Implants. 25(1):63–74.

Yang GL, He FM, Hu JA, Wang XX, Zhao SF. 2009. Effects of biomimetically and electrochemically deposited nano-hydroxyapatite coatings on osseointegration of porous titanium implants. Oral Surg Oral Med Oral Pathol Oral Radiol Endod. 107(6):782–789.